Bio-Plex® suspension array system

tech note 6488

Development and Validation of Bio-Plex Pro™ Human Chemokine Assays

Vinita Gupta, Richard Zimmerman, Terry Zhan, Tim Hamilton, Li Na, and Johnny Peng.

Protein Technology Research and Development Function Division, Bio-Rad Laboratories, Inc., 2000 Alfred Nobel Drive Hercules, CA 94547 USA

Introduction

The chemokine system belongs to a large family of inflammatory cytokines and receptors. Approximately 50 chemokines and 20 receptors have been identified and shown to play a critical role in tumor growth, inflammatory response, infection, autoimmune disorders, neoplasm, vascular diseases, and transplant rejection (Locati et al. 2005, Slettenaar and Wilson 2006). These low molecular weight (8–10 kD) proteins can be grouped into four chemokine subfamilies (C, CC, CXC, and CX_3C) according to the number of cysteine molecules and the spacing of cysteine residues (Figure 1). The C chemokines, called lymphotactins, are found in high levels in the spleen, thymus, intestine, and peripheral blood leukocytes. The CC chemokines have the first two cysteines in adjacent positions. They appear to attract monocytes, basophils, eosinophils, and lymphocytes, including NK cells. The CXC (where X denotes any amino acid) chemokines have the first two of four total cysteines separated by an amino acid. Most of them are chemo-attractants for neutrophils. The CX_3C chemokines include a single molecule with three amino acids between the first two cysteine residues. The only CX_3C chemokine discovered to date is fractalkine. It is both secreted and tethered to the surface of the cell that expresses it, thereby serving as both a chemo-attractant and an adhesion molecule.

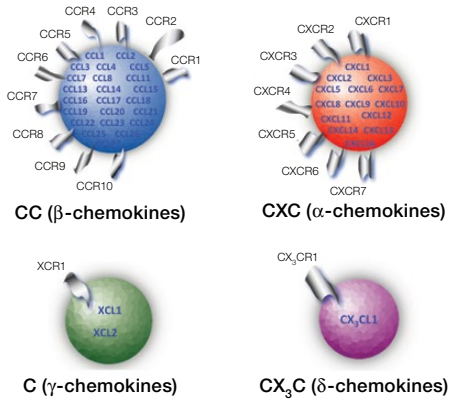

Fig. 1. Classification of chemokines and their respective receptors. Blue text refers to individual chemokines. Black text refers to receptors.

The regulatory functions of these chemokines are primarily exerted via binding to and signaling through specific chemokine receptors. The maintenance and fine-tuning of these functions is essential, and impairment of the entire chemokine system is often associated with various pathological processes. Many studies have found an association of chemokines and their receptors to specific diseases, leading to the development of novel and effective therapeutics. For example, chemokines, especially those involved in the inflammatory process, have long been connected with cancer; this connection has led to the development of chemokine receptor antagonists as therapeutic agents (Garin and Proudfoot 2011).

Maximizing assay throughput and studying interrelationships between several proteins in a single sample with a small sample volume is key for researchers studying these complex networks. In this study, we developed a panel of 40 magnetic bead–based chemokine assays using Luminex xMAP technology (Table 1) that are directly relevant to cancer biology, various inflammatory responses, and infectious diseases. The assays were validated according to performance criteria that are in agreement with standard bioanalytical guidelines. These criteria include assay range, sensitivity, precision, specificity, linearity of dilution, and parallelism to evaluate the robustness in key sample matrices. Magnetic beads were employed to enable automation of wash steps and to ensure compatibility with all Luminex-based life science research instruments.

Table 1. Bio-Plex Pro human chemokine 40-plex assay panel.

6Ckine/CCL21	IL-1β	MIF
BCA-1/CXCL13	IL-2	MIG/CXCL9
CTACK/CCL27	IL-4	MIP-1α/CCL3
ENA-78/CXCL5	IL-6	MIP-1δ/CCL15
Eotaxin/CCL11	IL-8/CXCL8	MIP-3α/CCL20
Eotaxin-2/CCL24	IL-10	MIP-3β/CCL19
Eotaxin-3/CCL26	IL-16	MPIF-1/CCL23
Fractalkine/CX3CL1	IP-10/CXCL10	SCYB16/CXCL16
GCP-2/CXCL6	I-TAC/CXCL11	SDF1α+β/CXCL12
GM-CSF	MCP-1/CCL2	TARC/CCL17
Gro-α/CXCL1	MCP-2/CCL8	TECK/CCL25
Gro-β/CXCL2	MCP-3/CCL7	TNF-α
I-309/CCL1	MCP-4/CCL13	
IFN-γ	MDC/CCL22	

BIO-RAD

Method

The Bio-Plex Pro human chemokine assays employ a standard sandwich enzyme immunoassay method using a 96-well plate format. The capture antibody–coupled beads are allowed to react with a sample containing the target of interest. After performing a series of washes to remove unbound materials, a biotinylated detection antibody specific for a different epitope on the target is added to the beads. The result is the formation of a sandwich of antibodies around the specific target. The reaction mixture is detected by the addition of a reporter dye, streptavidin-phycoerythrin (SA-PE), which binds to the sandwich complexes via the biotinylated detection antibodies. The contents of each well are drawn up into the Bio-Plex® array system, which identifies and quantifies each specific reaction based on bead color and fluorescence signal intensity. Data acquisition is performed using Bio-Plex 200 at low PMT setting, Bio-Plex 3D at the standard PMT setting, or Bio-Plex® MAGPIX™ system at the default setting (Table 2).

Table 2. Assay parameters.

	Samples + Capture Beads	Detection Antibody	SA-PE
Incubation time, min	60	30	10

	Shaker speed
RPM	850 ± 50

Instrument	PMT setting
Bio-Plex 200	Low RP1
Bio-Plex MAGPIX	Default
Bio-Plex 3D	Standard

Assay Performance

Assay specificity was examined by performing single-detection cross-reactivity weighted on standard point-3 in standard diluent. The study was conducted by testing the individual detection antibody in the presence of multiplexed antigens and capture beads. The degree of cross-reactivity is defined as the percentage of signal detected for the cross reactant relative to the specific signal for an analyte. With the exception of 6Ckine, eotaxin, GCP-2, fractalkine, Gro-α, and Gro-β, which showed mild cross-reactivity (1–2%) to selected assays, no cross-reactivity was detected in the rest of the panel.

Assay sensitivity, defined as the limit of detection (LOD), was determined by adding two standard deviations to the average of the median fluorescence intensity (MFI) for ten replicates of the standard curve blank (or RPMI media) run on three separate plates. The value was converted to a concentration as extrapolated from the standard curve. All assays except for 6Ckine, MIF, and SDF1α+β recorded <10 pg/ml. Precision was calculated by evaluating the MFI values of all eight standard points in triplicate over three independent runs. These runs were performed over a minimum of three days. The average of all coefficients of variance (%CV) of the calculated MFI of the three runs was reported for intra-assay precision. Comparable results were recorded in RPMI media. Inter-assay %CV was determined by the observed concentration of a 6-level spike control. Assay working range was defined as the point at which the intra-assay %CV for samples was ≤10%, with an accuracy of 70–130% (Table 3).

Assay accuracy (also defined as recovery) was calculated as the percentage of the observed concentration relative to the expected concentration. This parameter was evaluated in both multiplex and single-plex formats, in serum and RPMI media. The majority of the assays recovered 70–130% on at least six of the eight standard points. Selected standard curves, sample, and control measurement are shown in Figure 2.

Linearity of dilutions was examined by diluting spiked samples with the same serum or plasma matrix in a 1:3 serial dilution. High endogenous level analytes such as MIP-1δ, and non-spiked serum or plasma were diluted with sample diluent at a 1:4 serial dilution followed by twofold dilution with standard diluent in order to preserve the total serum content at each data point. The observed and expected sample concentrations within assay working ranges were plotted and the correlation coefficient (R^2) values were generated by performing linear regression analysis. Representative plots are shown in Figure 3. The study was conducted in both single- and multiplex formats.

Assay parallelism was investigated by comparing the slope of a sample curve (spiked and serially diluted serum or plasma samples) with a standard curve prepared in standard curve diluent. The purpose is to ensure the sample matrix is biologically comparable to the matrix of the standard curve. This was determined by calculating the slope difference between the two curves. Representative plots are shown in Figure 4.

Table 3. Assay sensitivity, precision, and assay working range in standard diluent and RPMI media.

	Limit of Detection (LOD), pg/ml		Assay Precision				Standard Diluent, pg/ml		RPMI, pg/ml	
			Mean Inter-assay, %CV		Mean Intra-assay, %CV					
Analyte	Standard Diluent	RPMI	Standard Diluent	RPMI	Standard Diluent	RPMI	LLOQ	ULOQ	LLOQ	ULOQ
6Ckine/CCL21	12.0	10.3	6	11	4	3	21.9	3,923	43.8	5,604
BCA-1/CXCL13	0.1	0.1	2	14	2	2	0.7	1,200	0.7	750
CTACK/CCL27	0.3	0.3	5	14	3	2	1.2	5,000	1.2	20,000
ENA-78/CXCL5	5.7	7.1	6	7	3	3	7.3	120,000	29.3	120,000
Eotaxin/CCL11	0.7	1.5	4	10	3	3	1.5	3,859	3.0	9,262
Eotaxin-2/CCL24	3.2	8.0	4	12	3	2	6.2	4,073	9.9	40,731
Eotaxin-3/CCL26	0.5	0.5	4	14	3	2	0.9	12,109	2.6	14,246
Fractalkine/CX3CL1	0.9	1.9	4	7	3	2	4.0	11,463	4.0	16,375
GCP-2/CXCL6	0.6	0.8	7	15	3	6	0.8	11,135	1.6	13,100
GM-CSF	1.0	0.5	3	3	4	2	5.3	35,000	2.1	35,000
Gro-α/CXCL1	4.2	5.5	4	5	2	2	3.1	7,024	24.9	12,770
Gro-β/CXCL2	2.7	4.9	8	8	3	2	4.6	13,257	18.5	18,939
I-309/CCL1	1.6	3.8	6	14	3	4	1.8	1,015	7.2	5,539
IFN-γ	0.4	0.1	5	14	3	3	2.3	20,236	1.3	5,502
IL-10	0.9	1.8	4	5	2	3	1.3	18,708	2.1	34,000
IL-16	0.8	0.3	6	4	3	3	2.1	34,000	2.6	7,000
IL-1β	0.1	0.1	4	5	2	2	0.4	7,000	0.8	13,000
IL-2	0.1	0.4	5	5	2	4	0.8	13,000	1.2	19,216
IL-4	1.0	0.6	4	5	3	3	1.2	4,804	0.7	750
IL-6	0.1	0.01	3	5	3	2	0.7	12,000	0.5	7,640
IL-8/CXCL8	0.04	0.3	4	4	3	2	0.5	7,640	1.6	26,832
IP-10/CXCL10	1.1	0.1	7	13	2	3	1.6	7,714	0.1	1,149
I-TAC/CXCL11	0.05	1.3	8	13	3	4	0.1	2,298	4.5	36,792
MCP-1/CCL2	0.1	0.0	3	3	3	3	0.3	4,812	0.3	4,812
MCP-2/CCL8	0.04	0.02	5	6	3	2	0.3	4,056	0.3	4,056
MCP-3/CCL7	1.3	1.1	6	8	6	4	1.9	20,133	11.1	30,389
MCP-4/CCL13	0.1	0.03	4	7	3	3	0.2	3,368	0.2	3,368
MDC/CCL22	0.5	1.3	3	6	3	4	0.9	14,649	14.3	14,649
MIF	15.4	467.2	7	13	2	5	23.1	377,724	46.1	377,724
MIG/CXCL9	1.1	2.0	7	6	3	3	1.8	19,600	14.4	29,585
MIP-1α/CCL3	0.3	0.3	6	6	4	2	0.4	1,543	0.4	1,543
MIP-1δ/CCL15	0.2	0.04	5	8	3	3	1.7	9,100	1.7	7,000
MIP-3α/CCL20	0.1	0.1	3	10	2	3	0.3	4,675	0.3	5,500
MIP-3β/CCL19	1.1	2.4	4	11	2	3	3.0	48,494	11.8	48,494
MPIF-1/CCL23	0.5	0.6	3	8	3	4	1.0	14,450	1.0	17,000
SCYB16/CXCL16	0.1	0.1	4	10	3	3	0.5	2,867	0.5	8,821
SDF1α+β/CXCL12	10.3	22.9	8	13	4	2	8.3	115,730	33.2	68,077
TARC/CCL17	1.1	2.6	5	8	4	3	1.7	430	10.1	3,439
TECK/CCL25	4.9	6.8	5	12	4	2	20.6	114,493	16.4	134,698
TNF-α	0.2	0.5	8	5	3	3	0.9	13,879	0.9	13,879

Note: LLOQ, lower limit of quantification; ULOQ, upper limit of quantification

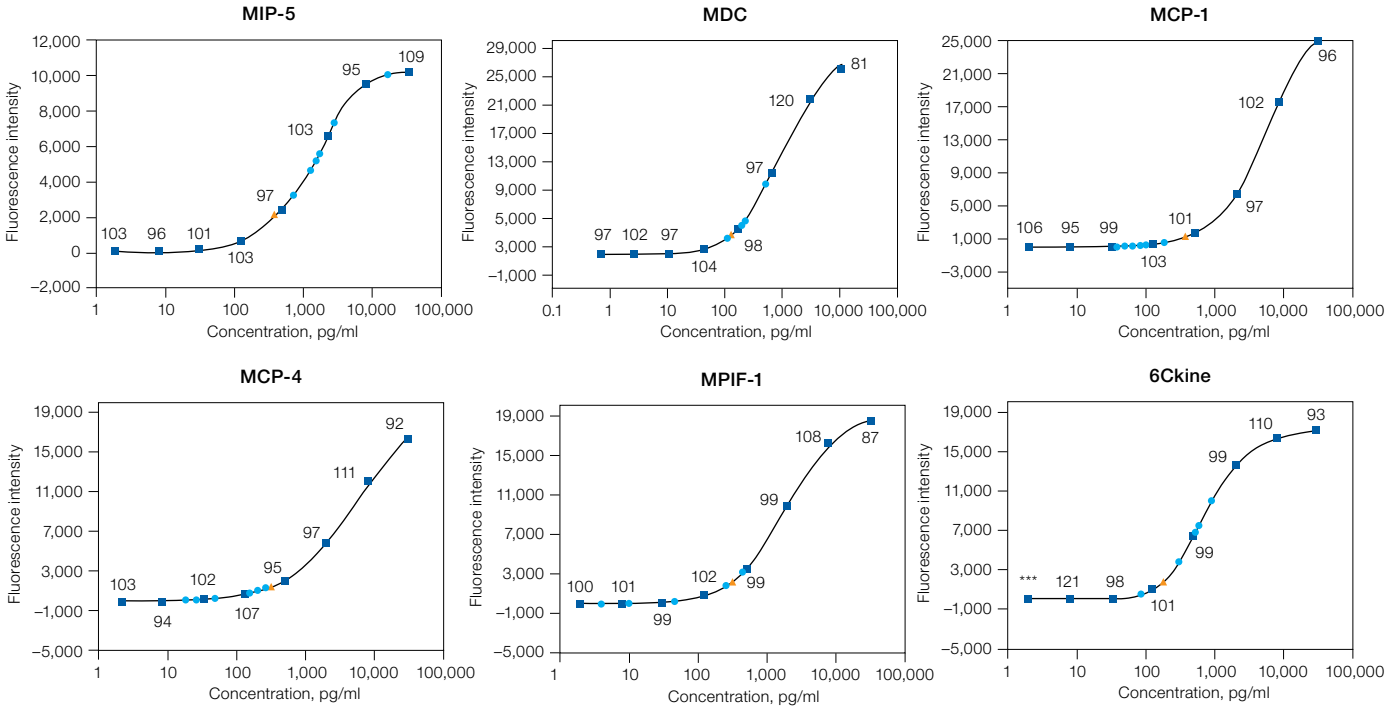

Fig. 2. Representative standard curves. Standard with % recovery (■); control (▲); unknown (●). ***, standard recovery undefined.

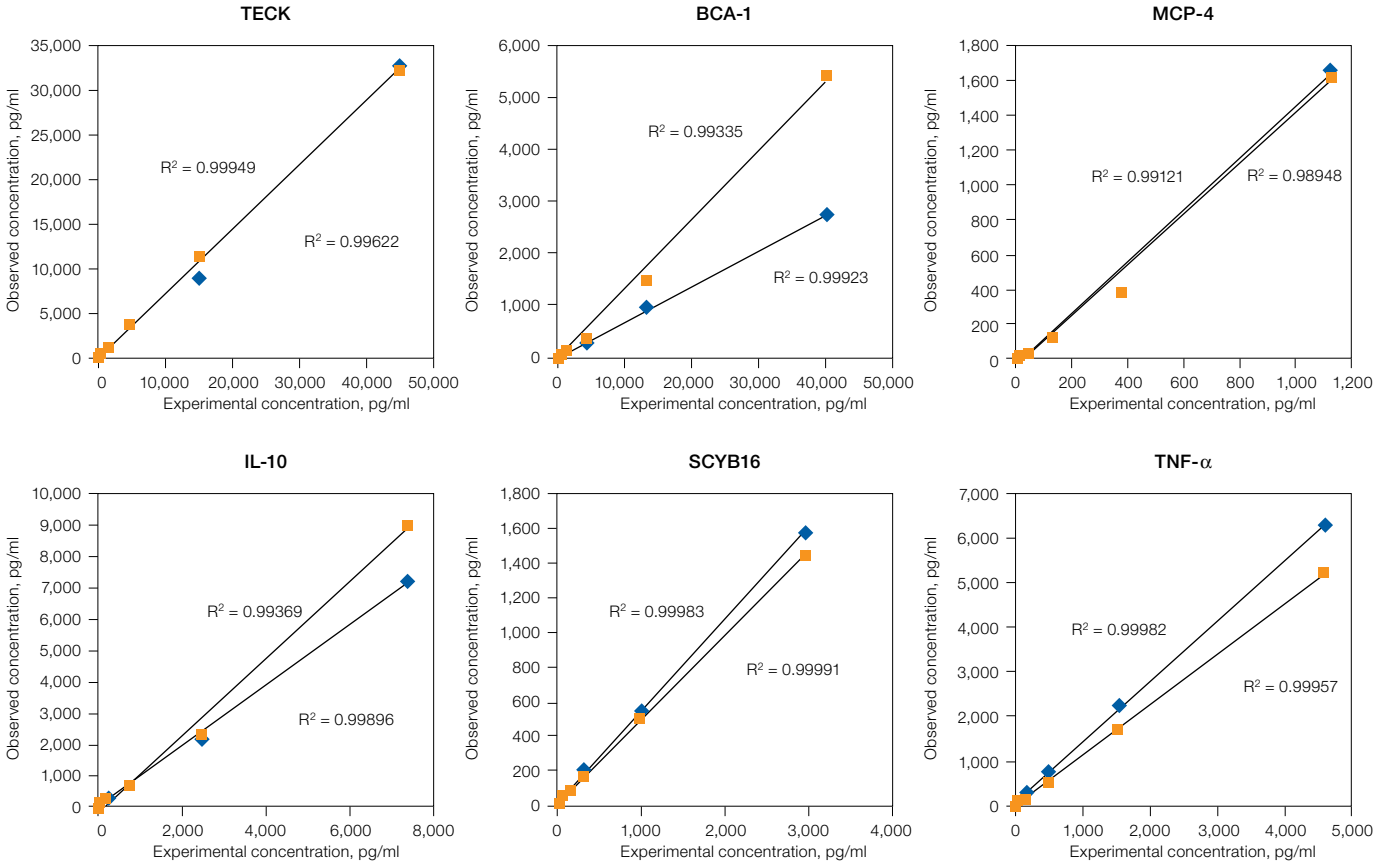

Fig. 3. Linearity of dilution in serum and plasma matrices. Samples with high endogenous levels or spiked samples were serially diluted to obtain at least four data points. The observed and expected analyte concentrations were plotted and the correlation coefficient (R^2) values reflect linearity in signal response. Plasma (◆); serum (■).

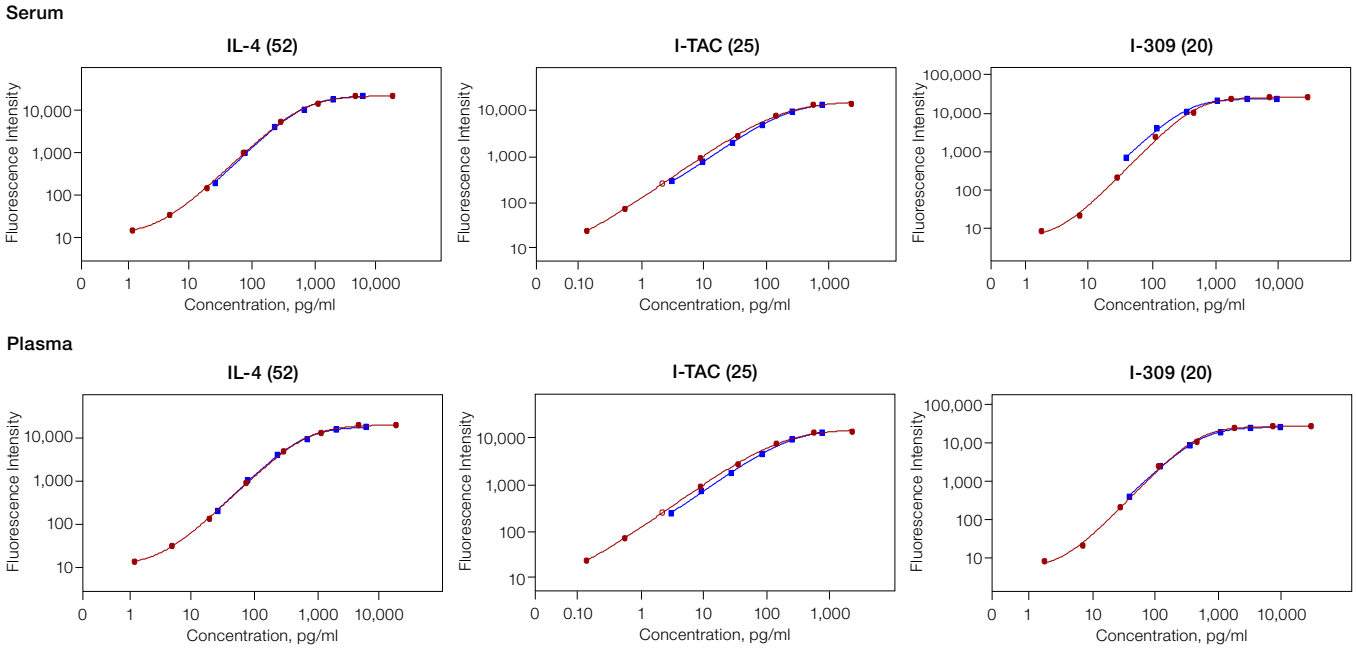

Fig. 4. Assay parallelism. Standard curve (—) and serial dilution of a spiked or neat sample (—).

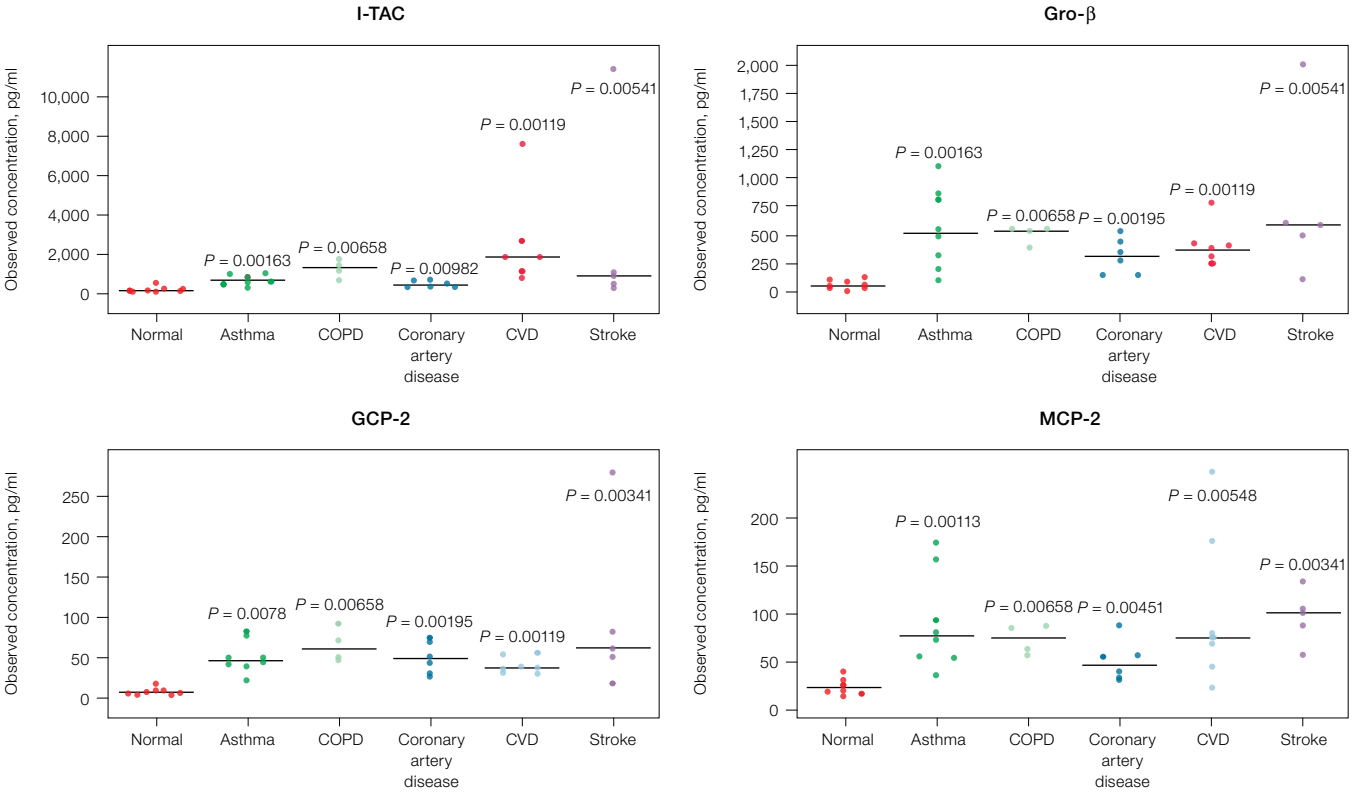

Fig. 5. Chemokine levels in normal and diseased serum. Dot plots with *P* values were generated using the Bio-Plex Data Pro™ software. *P* values <0.05 indicate significant difference between normal vs. disease state.

Validation with Biological Samples

The chemokine assays were validated with serum and plasma, tissue culture supernatant, and cell lysate samples. Serum levels of individuals with asthma, chronic obstructive pulmonary disease, cardiovascular disease, and stroke are summarized in Figure 5. Representative THP-1 cell lysate performance data is shown in Figure 6. Selected tissue culture supernatant results are shown in Figure 7.

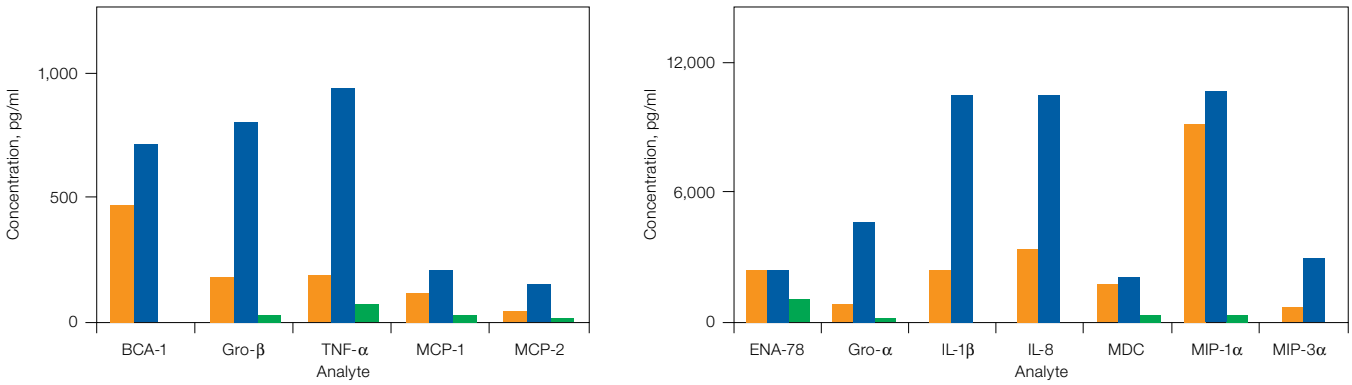

Fig. 6. Chemokine levels in human THP-1 monocytic cell lysate. The cells were challenged for three days with LPS (10 µg/ml) and a combination of LPS and Con-A at 10 µg/ml. Cell lysate was prepared using the Bio-Plex cell lysis kit. LPS (■); LPS + ConA (■); untreated (■).

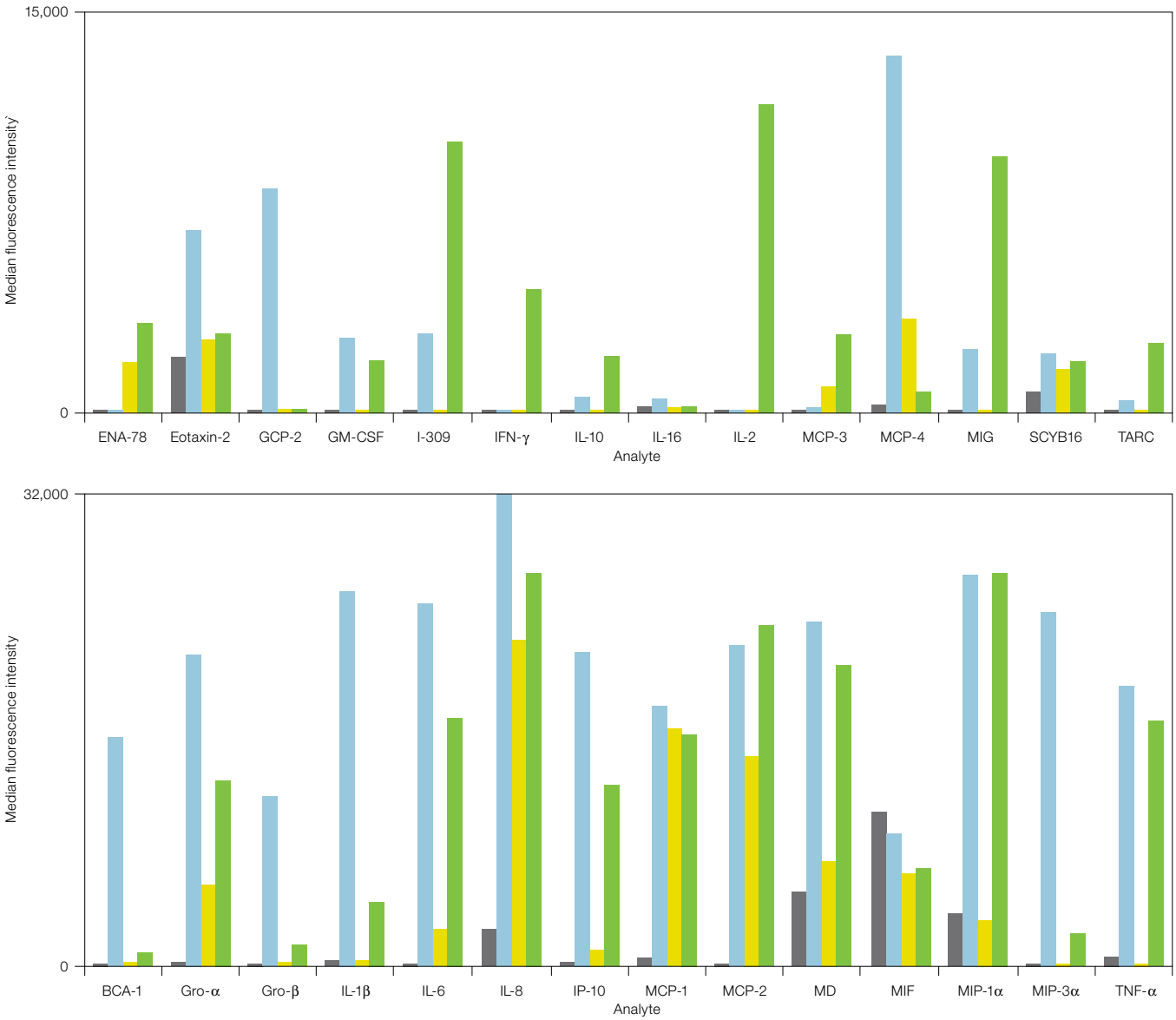

Fig. 7. Chemokine profile in tissue culture supernatant. Human THP-1 monocytic cells were challenged with a combination of LPS and Con-A at 10 µg/ml. PBMC isolated from human blood was stimulated with a combination of PMA (50 ng/ml), ionmycin (1 µg/ml), PHA (5 µg/ml), and Con-A (10 µg/ml). The resulting cell culture supernatant was harvested three days after stimulation and used for the determination of chemokines. Untreated THP-1 cells and PBMC were used as controls for each condition. Untreated THP-1 (■); THP-1 + LPS + ConA (■); untreated PBMC (■); PBMC + PMA + ionmycin + PHA + ConA (■).

Agreement among xMAP Platforms — Bio-Plex MAGPIX, Bio-Plex 200, and Bio-Plex 3D Systems

The assays were evaluated on Bio-Plex MAGPIX, Bio-Plex 200, and Bio-Plex 3D systems in all key sample matrices. Overall, excellent agreement in sample readout was recorded on all three platforms (Figure 8).

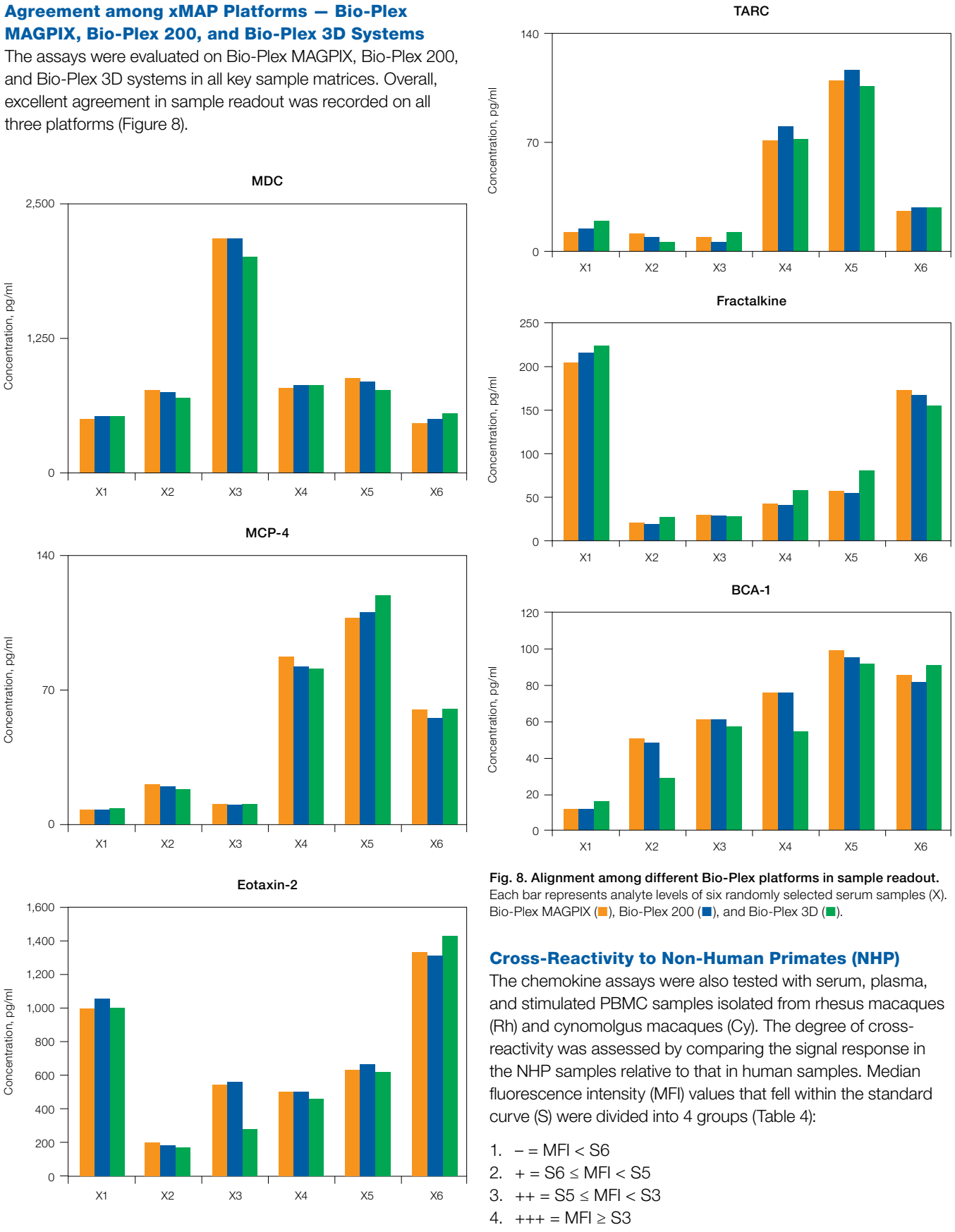

Fig. 8. Alignment among different Bio-Plex platforms in sample readout. Each bar represents analyte levels of six randomly selected serum samples (X). Bio-Plex MAGPIX (■), Bio-Plex 200 (■), and Bio-Plex 3D (■).

Cross-Reactivity to Non-Human Primates (NHP)

The chemokine assays were also tested with serum, plasma, and stimulated PBMC samples isolated from rhesus macaques (Rh) and cynomolgus macaques (Cy). The degree of cross-reactivity was assessed by comparing the signal response in the NHP samples relative to that in human samples. Median fluorescence intensity (MFI) values that fell within the standard curve (S) were divided into 4 groups (Table 4):

1. – = MFI < S6
2. + = S6 ≤ MFI < S5
3. ++ = S5 ≤ MFI < S3
4. +++ = MFI ≥ S3

Table 4. Cross-reactivity to non-human primates.

Analyte	Cynomolgous	Rhesus
6Ckine/CCL21	–	–
BCA-1/CXCL13	+++	+++
CTACK/CCL27	–	–
ENA-78/CXCL5	+	+
Eotaxin/CCL11	+	+
Eotaxin-2/CCL24	–	–
Eotaxin-3/CCL26	–	–
Fractalkine/CX3CL1	+++	+
GCP-2/CXCL6	–	–
GM-CSF	+++	+++
Gro-α/CXCL1	–	–
Gro-β/CXCL2	+	+
I-309/CCL1	–	–
IFN-γ	–	–
IL-10	+++	+++
IL-16	+	+
IL-1β	+++	+++
IL-2	–	–
IL-4	++	+
IL-6	+++	+++
IL-8/CXCL8	+++	+++
IP-10/CXCL10	+++	+++
I-TAC/CXCL11	+++	+++
MCP-1/CCL2	+++	+++
MCP-2/CCL8	++	++
MCP-3/CCL7	–	–
MCP-4/CCL13	+++	+++
MDC/CCL22	+	–
MIF	+++	+++
MIG/CXCL9	–	–
MIP-1α/CCL3	+++	+++
MIP-1δ/CCL15	–	+
MIP-3α/CCL20	–	–
MIP-3β/CCL19	++	++
MPIF-1/CCL23	–	–
SCYB16/CXCL16	–	+
SDF1α+β/CXCL12	+	+
TARC/CCL17	–	–
TECK/CCL25	+	+
TNF-α	+	+

Note: Serum, plasma, and supernatants from cultured PBMC samples were collected from cynomolgus macaques and rhesus macaques. The PBMC samples were stimulated by three mitogen treatments: (a) PMA (50 ng/ml)/ionmycin (1 µg/ml); (b) Con-A (10 µg/ml); (c) PMA (50 ng/ml)/ionmycin (1 µg/ml)/PHA (5 µg/ml)/Con-A (10 µg/ml). Cell culture supernatants were harvested 72 hours after stimulation and used for the determination of chemokines. Supernatant from unstimulated PBMC was used as control.

Conclusions

In this study, we developed and validated a new Bio-Plex Pro chemokine panel for quantifying 40 human cytokines in one sample. This is a significant advantage for researchers collecting combinatorial chemokine information with a limited sample volume. The assays have been validated in different matrices, as well as in biological samples, and have been shown to fall under performance criteria that are in agreement with standard bioanalytical guidelines. These multiplex chemokine assays have been optimized for high precision and lot-to-lot reproducibility of sample measurement, guided by a single-level quality control. The capacity to multiplex in a small sample volume provides an effective option over the traditional ELISA method. The assays are ideal for evaluating chemokines as new biomarkers of interest in cancer pathology as well as therapeutic targets for various inflammatory disorders.

References

Garin A and Proudfoot AEJ (2011). Chemokines as targets for therapy. Exp Cell Res 317, 602–612.

Locati M et al. (2005). Chemokines and their receptors: Roles in specific clinical conditions and measurement in the clinical laboratory. Am J Clin Pathol 123 (Suppl 1), S82–S95.

Slettenaar VIF and Wilson JL (2006). The chemokine network: A target in cancer biology? Adv Drug Delivery Rev 58, 962–974.

BIO-RAD

Bio-Rad Laboratories, Inc.

Life Science Group

Web site *www.bio-rad.com* ***USA*** *800 424 6723* ***Australia*** *61 2 9914 2800* ***Austria*** *01 877 89 01* ***Belgium*** *09 385 55 11* ***Brazil*** *55 11 3065 7550* ***Canada*** *905 364 3435* ***China*** *86 21 6169 8500* ***Czech Republic*** *420 241 430 532* ***Denmark*** *44 52 10 00* ***Finland*** *09 804 22 00* ***France*** *01 47 95 69 65* ***Germany*** *089 31 884 0* ***Greece*** *30 210 9532 220* ***Hong Kong*** *852 2789 3300* ***Hungary*** *36 1 459 6100* ***India*** *91 124 4029300* ***Israel*** *03 963 6050* ***Italy*** *39 02 216091* ***Japan*** *81 3 6361 7000* ***Korea*** *82 2 3473 4460* ***Mexico*** *52 555 488 7670* ***The Netherlands*** *0318 540666* ***New Zealand*** *64 9 415 2280* ***Norway*** *23 38 41 30* ***Poland*** *48 22 331 99 99* ***Portugal*** *351 21 472 7700* ***Russia*** *7 495 721 14 04* ***Singapore*** *65 6415 3188* ***South Africa*** *27 861 246 723* ***Spain*** *34 91 590 5200* ***Sweden*** *08 555 12700* ***Switzerland*** *026 674 55 05* ***Taiwan*** *886 2 2578 7189* ***Thailand*** *1800 88 22 88* ***United Kingdom*** *020 8328 2000*